

# The Effect of $\epsilon$ -FeSi and Si Content on the Physical and Thermoelectric Properties of $\text{FeSi}_x$ Compound

## ผลของ $\epsilon$ -FeSi และปริมาณ Si ต่อสมบัติทางกายภาพและสมบัติทางเทอร์โมอิเล็กทริกของสารประกอบ $\text{FeSi}_x$

อาภาภรณ์ สกฤตกระเวก<sup>1,\*</sup> และ สมชาย เกียรติกมลชัย<sup>2</sup>

<sup>1</sup> ภาควิชาฟิสิกส์ คณะวิทยาศาสตร์ สถาบันเทคโนโลยีพระจอมเกล้าเจ้าคุณทหารลาดกระบัง

<sup>2</sup> ภาควิชาฟิสิกส์ คณะวิทยาศาสตร์ จุฬาลงกรณ์มหาวิทยาลัย

\*Email: ksaparp@kmitl.ac.th



### บทคัดย่อ

สารประกอบเหล็ก-ซิลิกอน ถูกเตรียมจากการผสมผงเหล็กและซิลิกอน โดยมีอัตราส่วนของเหล็กต่อซิลิกอนเป็น 1:2.0 1:2.3 และ 1:2.5 ผงที่ผสมถูกนำไปเผาที่อุณหภูมิ 1550 °C ภายใต้บรรยากาศของอาร์กอน การเปลี่ยนเฟสถูกวิเคราะห์โดยใช้ XRD, DTA, EDS, และ SEM ค่าเทอร์โมอิเล็กทริกพาวเวอร์และสภาพนำไฟฟ้าถูกวัดโดยเครื่อง ZEM-2 หลังการเผา สารตัวอย่างที่มีอัตราส่วนของเหล็กต่อซิลิกอนเป็น 1:2.0 และ 1:2.3 จะพบโครงสร้างของ  $\epsilon$ -FeSi กระจายอยู่ในโครงสร้างของ  $\alpha$ -Fe<sub>2</sub>Si<sub>5</sub> สำหรับสารตัวอย่างที่มีอัตราส่วนของเหล็กต่อซิลิกอนเป็น 1:2.5 จะพบโครงสร้างของ  $\epsilon$ -Fe<sub>2</sub>Si<sub>5</sub> เพียงโครงสร้างเดียว การปรากฏอยู่ของโครงสร้าง  $\epsilon$ -FeSi ส่งผลต่อเส้นโค้ง DTA อย่างมาก ค่าเทอร์โมอิเล็กทริกพาวเวอร์ของสารตัวอย่างทุกชิ้นภายหลังการเผาจะมีค่าต่ำ (ต่ำกว่า 10  $\mu\text{V/K}$ ) โครงสร้าง  $\alpha$  และ  $\epsilon$  จะค่อยๆ เปลี่ยนไปเป็นโครงสร้างของสารกึ่งตัวนำ  $\beta$ -FeSi<sub>2</sub> โดยการอบที่อุณหภูมิ 830 °C หรือ 960 °C ซึ่งเป็นอุณหภูมิที่เกิดปฏิกิริยายุทเทคทอย ( $\alpha \rightarrow \beta + \text{Si}$ ) และเพอริเทคทอย ( $\alpha + \epsilon \rightarrow \beta$ ) การกระจายของซิลิกอนในโครงสร้างของสารตัวอย่างทำให้ค่าเทอร์โมอิเล็กทริกพาวเวอร์เพิ่มขึ้นอย่างมากโดยเฉพาะที่อุณหภูมิต่ำ (ต่ำกว่า 400 °C) ในขณะที่การปรากฏโครงสร้างโลหะ  $\epsilon$  ทำให้สภาพนำไฟฟ้าเพิ่มขึ้นอย่างมาก ค่าพาวเวอร์แฟกเตอร์ที่สูงที่สุดเท่ากับ  $2.86 \times 10^{-5} \text{ W}/(\text{m}\cdot\text{K}^2)$  ที่อุณหภูมิ 600 °C ของสารตัวอย่าง  $\text{FeSi}_{2.3}$

คำสำคัญ: 

$\beta$ -FeSi<sub>2</sub>  $\epsilon$ -FeSi วัสดุเทอร์โมอิเล็กทริก เพาเวอร์แฟกเตอร์



### Abstract

Bulk iron-silicon compound was prepared from a mixture of Fe and Si powder with Fe/Si atomic ratios 1:2.0, 1:2.3 and 1:2.5. The mixture was heated up to 1550 °C under the argon-flow

atmosphere. Phase transitions were investigated using XRD, DTA, EDS, and SEM. The thermoelectric power and electrical conductivity were measured by ZEM-2. As-grown samples consisted of  $\epsilon$ -FeSi dispersing into  $\alpha$ -Fe<sub>2</sub>Si<sub>5</sub> matrix for Fe/Si atomic ratios 1:2.0 and 1:2.3. For Fe/Si atomic ratio 1:2.5 only  $\alpha$ -Fe<sub>2</sub>Si<sub>5</sub> existed. The absence of  $\epsilon$ -phase greatly affected the DTA curves. Thermoelectric power of all as-grown samples was relatively low (less than 10  $\mu$ V/K).  $\alpha$  and  $\epsilon$  phases were gradually transformed into a semiconducting  $\beta$ -FeSi<sub>2</sub> phase by subsequent isothermal annealing at 830 °C or 960 °C. The eutectoid reaction ( $\alpha \rightarrow \beta + \text{Si}$ ) and peritectoid reaction ( $\alpha + \epsilon \rightarrow \beta$ ) occurred at these temperatures. The dispersion of excess Si markedly increased the thermoelectric power especially at low temperature (less than 400 °C) while the present of metallic  $\epsilon$ -phase markedly increased the electrical conductivity. The maximum power factor is as high as  $2.86 \times 10^{-5}$  W/(m.K<sup>2</sup>) at 600 °C for FeSi<sub>2,3</sub> sample.

### Keywords:

$\beta$ -FeSi<sub>2</sub>,  $\epsilon$ -FeSi, thermoelectric material, power factor

## 1. Introduction

The term of thermoelectric material is referred to a material which exhibits substantial thermoelectric effects. The thermoelectric effect is a direct conversion of temperature difference to electric voltage and vice versa. The power factor is one of parameters that commonly used to evaluate the performance of thermoelectric materials. The power factor is determined by

$$P = \alpha^2 \sigma$$

where  $\alpha$  is the thermoelectric power and  $\sigma$  is the electrical conductivity. It is clear from this equation that in order to obtain a high power factor, a large thermoelectric power and electric conductivity are required.

The stoichiometric phase of iron disilicide ( $\beta$ -FeSi<sub>2</sub>) is one of the most potential thermoelectric

material candidates, due to its low cost of raw material, high oxidation resistance, non-toxicity and high operating temperature up to 970 °C [1,2]. The equilibrium phase diagram (Fig. 1) shows the stoichiometric composition of  $\beta$ -FeSi<sub>2</sub> and eutectic of  $\epsilon$ -FeSi and  $\alpha$ -Fe<sub>2</sub>Si<sub>5</sub>. Those high-temperature,  $\epsilon$ -phase and  $\alpha$ -phase, are metallic and they have good electrical conductivity and but very low thermoelectric power. The  $\beta$ -FeSi<sub>2</sub> phase, which shows high thermoelectric power as a semiconductor phase, is formed by the following three reactions;

1. the peritectoid reaction ( $\alpha + \epsilon \rightarrow \beta$ ) at 982 °C,
2. the eutectoid reaction ( $\alpha \rightarrow \beta + \text{Si}$ ) at 937 °C, and
3. the subsequent reaction ( $\epsilon + \text{Si} \rightarrow \beta$ ) [3,4].

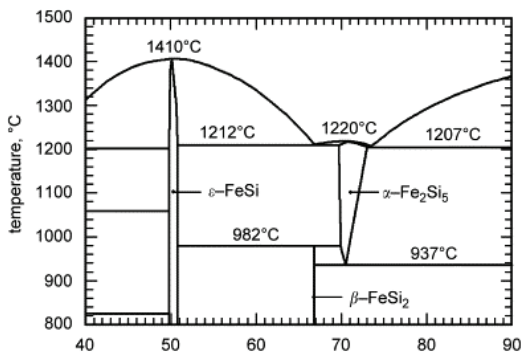


Figure 1. Equilibrium Fe-Si binary phase diagram [5].

Bulk  $\beta$ - $\text{FeSi}_2$  is conventionally produced by melting iron and silicon in argon atmosphere and then cooled down to room temperature. Alloy obtained after melting contained  $\alpha$ - and  $\epsilon$ -phase [5]. Sample was grinded into powder by mechanical alloying (MA) or mechanical ground (MG) process. The MA was found to be suitable for the production of Fe-Si powders [6, 7]. Umemoto et al. [6] suggested at least 500 h of milling to induce  $\beta$ - $\text{FeSi}_2$  transformation by MA. Hot-pressed (HP) or spark plasma sintering (SPS) was used to improve the densification of sample [8]. The powders were successfully consolidated by HP and it obtained the relatively high density sample (97% of theoretical density) [7]. The high density compact was shown to consist of the untransformed mixture of  $\epsilon$ - and  $\alpha$ -phase. Finally, the sample was annealed for enhance the  $\beta$ -phase formation. This annealing for  $\beta$ -phase formation requires a long time

period, because kinetic for this conversion has been known to be sluggish [9]. Cu addition was used to increase the rate formation of  $\beta$ -phase [5,10] but Cu content caused a deterioration of thermoelectric power [10]. The finely dispersed of second phases in  $\beta$ -matrix can be improved thermoelectric properties by reducing the thermal conductivity due to phonon scattering [11,12]. Hirochi Nagai et al. [11] reported that small SiC particles about 20 nm in size were effective to reducing the thermal conductivity. The new compositions of  $\text{Fe}_2\text{Si}_5$  were prepared instead of  $\text{FeSi}_2$  because  $\epsilon$ -phase not formed in the as grown sample [13] and it is expected that excess Si particle from eutectoid reaction ( $\alpha \rightarrow \beta + \text{Si}$ ) will disperse in  $\beta$ -matrix and it may act as preferred scattering center [2]. The purpose of this work was to study and discuss the effect of  $\epsilon$ -FeSi phase on the qualitative reaction in  $\text{FeSi}_x$  as presented in DTA curve where  $x = 2.0, 2.3$  and  $2.5$ . Furthermore, we studied the effect of  $\epsilon$ -FeSi and Si dispersion on thermoelectric power and electrical conductivity.

## 2. Material and method

### 2.1 Sample preparation

A mixture of Fe and Si powders with Fe/Si atomic ratio 1:2.0, 1:2.3 and 1:2.5 were used. The mixed powders were melted in an alumina

crucible coated with boron nitride releasing agent.

The crucible was put inside a tube furnace which has the argon gas flowing at the rate of 100 cc/min. The powder was heated up to 800 °C at the rate of 8 °C/min, and then to 1550 °C at the rate of 5 °C/min. The molten material was held for 1 h at this temperature. After cooling at the rate of 5 °C/min to room temperature, samples were cut into slices with a thickness of approximately 1.7 mm and polished. Impurity on samples surface were removed by washing with alcohol and deionized water. Three types ( $\text{FeSi}_{2.0}$ ,  $\text{FeSi}_{2.3}$ ,  $\text{FeSi}_{2.5}$ ) of samples were ex-situ annealed at 830 °C or 960 °C for 12 h.

## 2.2 Characterization

Structural property of the sample was identified by X-ray diffraction (XRD). The morphology of the sample was observed by BEI (back-scattered electron image) of scanning electron microscope (SEM). The composition of Fe and Si in the sample were determined with an energy-dispersive X-ray analysis (EDS). The cyclic heating and cooling in the temperature range between 600 °C and 1050 °C at the rate of 10 °C/min were carried out by using a differential thermal analysis (DTA) to examine the transformation behavior. The thermoelectric power and electrical conductivity were measured by DC four-terminal method (ZEM-2, Ulvac, Inc.) over the temperature range of 30 – 700 °C.

## 3. Results and Discussion

### 3.1 Structural properties of as-grown sample

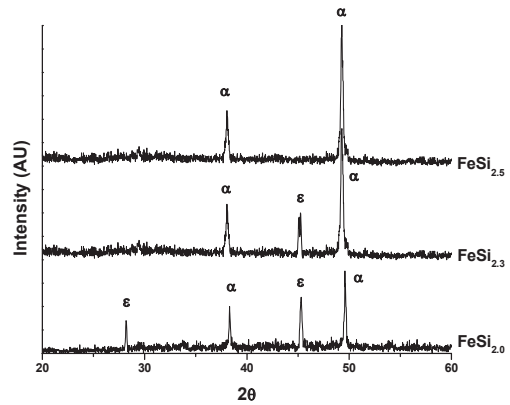


Figure 2. XRD patterns of as-grown samples.

Fig. 2 shows XRD patterns of as-grown samples  $\text{FeSi}_{2.0}$ ,  $\text{FeSi}_{2.3}$  and  $\text{FeSi}_{2.5}$ . Samples  $\text{FeSi}_{2.0}$  and  $\text{FeSi}_{2.3}$  consisted of  $\epsilon$ - and  $\alpha$ -phases while sample  $\text{FeSi}_{2.5}$  consisted of only  $\alpha$ -phase. The elemental Si ( $2\theta \approx 28.4^\circ$ ) and Fe ( $2\theta \approx 44.8^\circ$ ) peak disappeared after 1 h melting at 1550 °C. The presence of the  $\alpha$ - and  $\epsilon$ -phase in the sample  $\text{FeSi}_{2.0}$  with starting sample of Fe-Si with 1:2.0 atomic ratio means that  $\beta$ -phase is not formed from the melt. So, annealing for  $\beta$ -phase formation is required after solidification. SEM images were shown in Fig.3.

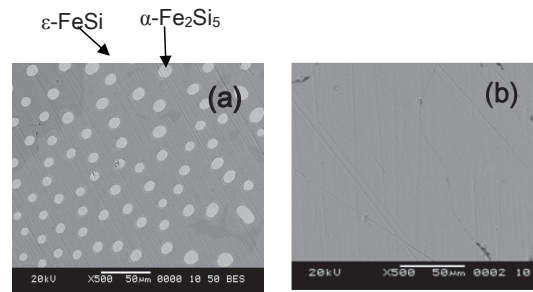


Figure 3. SEM images of as-grown samples (a)  $\text{FeSi}_{2.0}$  and (b)  $\text{FeSi}_{2.5}$ .

## The Effect of $\epsilon$ -FeSi and Si Content on the Physical and Thermoelectric Properties of $\text{FeSi}_x$ Compound

From EDS spectrum, the Fe:Si atomic ratio was 1:1.0 for the white part which agrees with the stoichiometric composition of  $\epsilon$ -FeSi. The shape of  $\epsilon$  phase is mostly rounded with the diameter about 10  $\mu\text{m}$ . For the dark matrix, the Fe:Si ratio was 1:2.5 which is equivalent to the stoichiometric composition of  $\alpha$ - $\text{Fe}_2\text{Si}_5$ . Some crack was occurred due to cutting and polishing.

### 3.2 DTA measurement

According to the phase transformation reaction, other phase of as-grown sample can be changed to  $\beta$ -phase by thermal treatment. DTA was also carried out to obtain qualitative information of  $\beta$ -phase formation. For samples  $\text{FeSi}_{2.0}$  and  $\text{FeSi}_{2.3}$ , there were two endothermic peaks at temperature rang 960–975  $^\circ\text{C}$  and 1010  $^\circ\text{C}$  for all heating stages and one broad exothermic peak at 830  $^\circ\text{C}$  for all cooling stages. For sample  $\text{FeSi}_{2.5}$ , there was only one sharp endothermic peak at 960  $^\circ\text{C}$  for the heating stage, no peak for cooling stage. Further heating or cooling stages did not change the DTA curves.

Isothermal annealing at 830  $^\circ\text{C}$  led to the semiconducting  $\beta$ -phase transformation by peritectoid reaction ( $\epsilon + \alpha \rightarrow \beta$ ) [13]. The peritectoid reaction did not occur in as-grown sample  $\text{FeSi}_{2.5}$  because there was no  $\epsilon$ -phase presented and so the exothermic peak at 830  $^\circ\text{C}$  vanished. For samples  $\text{FeSi}_{2.0}$  and  $\text{FeSi}_{2.3}$ , the degree of peritectoid reaction was slow and showed broadening exothermic peak. The first endothermic peak for 1st heating stage of samples  $\text{FeSi}_{2.0}$  and  $\text{FeSi}_{2.3}$  occurred at at 960  $^\circ\text{C}$  in

sample  $\text{FeSi}_{2.5}$ , where initial sample contained only  $\alpha$ -phase, for all heating stages. 960  $^\circ\text{C}$  and it shifted to higher temperatures for 2<sup>nd</sup> and 3<sup>rd</sup> heating stages (at temperature range 960–975  $^\circ\text{C}$ ).

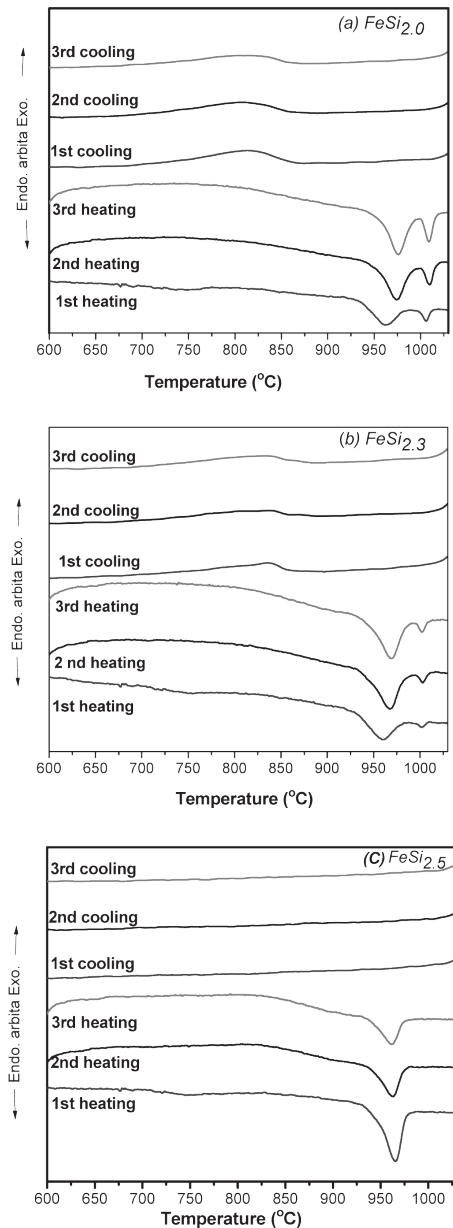


Figure 4. DTA curves of (a) sample  $\text{FeSi}_{2.0}$ , (b) sample  $\text{FeSi}_{2.3}$  and (c) sample  $\text{FeSi}_{2.5}$ .

It was interesting to note that this peak also existed. This endothermic peak at 960 °C corresponds to the eutectoid reaction ( $\alpha \rightarrow \beta + \text{Si}$ ). This reaction had been confirmed by SEM images (Fig. 5b and 5c), the structure shows Si network from eutectoid reaction disperse in the  $\beta$  matrix. Samples  $\text{FeSi}_{2.0}$  and  $\text{FeSi}_{2.3}$  had  $\epsilon$ - and  $\alpha$ -phases, the peritectoid reaction ( $\alpha + \epsilon \rightarrow \beta$ ) appears at 986 °C [3], quite close to the reported 975 °C. Therefore, the temperature range 960–975 °C consists of both peritectoid and eutectoid reactions. As-grown sample  $\text{FeSi}_{2.5}$  had no  $\epsilon$ -phase, only eutectoid reaction occurred at 960 °C.

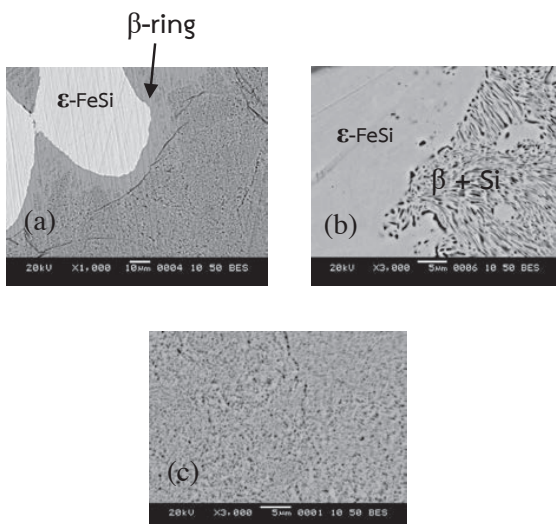


Figure 5. Microstructure of annealed samples.  
 (a) Sample  $\text{FeSi}_{2.0}$  annealed at 830 °C ;  
 (b) Sample  $\text{FeSi}_{2.3}$  annealed at 960 °C;  
 (c) Sample  $\text{FeSi}_{2.5}$  annealed at 960 °C.

The endothermic peak at 1010 °C for sample  $\text{FeSi}_{2.0}$  became broader for sample  $\text{FeSi}_{2.3}$  and disappeared for sample  $\text{FeSi}_{2.5}$ . This implies that this peak must be associated with the  $\epsilon$ -phase. This peak has been known as a reverse reaction of peritectoid reaction ( $\beta \rightarrow \alpha + \epsilon$ ) [14,15].

### 3.3 Structural properties and thermoelectric power of annealed-sample

Samples were annealed at 830 °C or 960 °C for 12 h according to the DTA result. Yamauchi et al. [5] reported that the  $\beta$ -phase formation from peritectoid reaction gave the ring-like structure surrounding  $\epsilon$ -phase while the eutectoid structure gave the lamellar structure composed of  $\beta$  and Si phase. Fig. 5 shows microstructure of annealed samples. In case of annealing at 830 °C, we can see little  $\beta$ -phase layer forming around the  $\epsilon$ -phase by peritectoid reaction. When sample was annealed at 960 °C, its structure showed a network of Si from the eutectoid reaction dispersing in the  $\beta$  matrix. XRD patterns of annealed samples are shown in Fig. 6 and  $\beta$ -phase is clearly seen in all annealed samples. For sample  $\text{FeSi}_{2.5}$ , Si peak is also present significantly as a result of strong eutectoid reaction.  $\epsilon$ -phase could not be observed from XRD pattern, despite its presence in SEM micrograph of all annealed sample. This might be due to smaller  $\epsilon$ -phase quantity than a detectable limit of XRD machine.



## The Effect of $\epsilon$ -FeSi and Si Content on the Physical and Thermoelectric Properties of $\text{FeSi}_x$ Compound

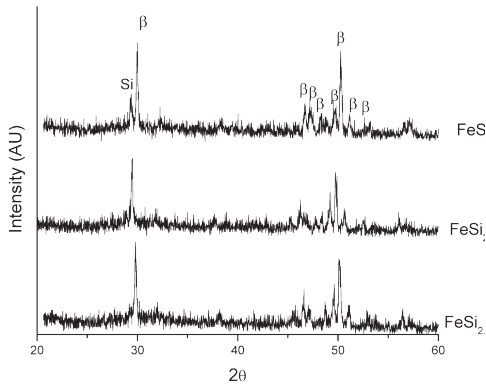


Figure 6. XRD patterns of annealed samples.

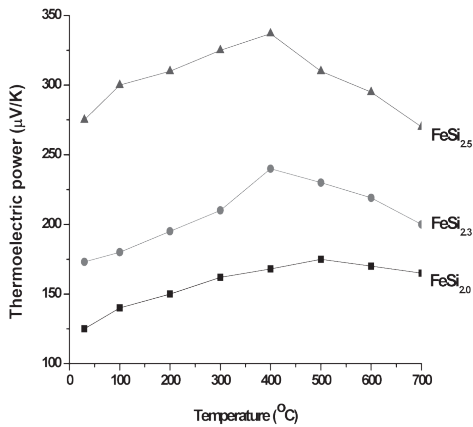


Figure 7: Temperature dependence of thermoelectric power of  $\text{FeSi}_{2.0}$ ,  $\text{FeSi}_{2.3}$  and  $\text{FeSi}_{2.5}$ .

In this work, the thermoelectric power is positive for all compositions, mean that hole-like carrier dominates the transport. Unintentional doping of sample was due to the unknown impurity in raw materials and boron nitride releasing agent used. Zhengxin Liu et al. [15] studied the effect of doping  $\beta$ - $\text{FeSi}_2$  thin film with boron and arsenic by sputtering method. The results indicated that the  $\beta$ - $\text{FeSi}_2$  thin film doped with boron was p-type.

Figure 7 shows the temperature dependence of the thermoelectric power for  $\text{FeSi}_{2.0}$ ,  $\text{FeSi}_{2.3}$  and  $\text{FeSi}_{2.5}$  samples over the temperature range of 30 – 700 °C. The thermoelectric power increases with increasing temperature and then decreases at high temperature. The marked decrease in the thermoelectric power at high temperature is due to the marked increase in the carrier concentration. The thermoelectric power of the  $\text{FeSi}_{2.5}$  samples are significantly higher than that of the  $\text{FeSi}_{2.0}$  and  $\text{FeSi}_{2.3}$  samples. This result can be explained by two reasons, the existence of metallic  $\epsilon$ -phase in annealed  $\text{FeSi}_{2.0}$  and  $\text{FeSi}_{2.3}$  samples as presented in SEM images and the influence of excess Si on the carrier scattering. The thermoelectric power of the  $\text{FeSi}_{2.3}$  sample is larger than  $\text{FeSi}_{2.0}$  sample. This is due to the small excess Si particle in  $\text{FeSi}_{2.3}$  promotes the value of thermoelectric power. At temperature below 400 °C, the thermoelectric power of all samples are largely composition dependence. The difference in thermoelectric power of all samples decreases with increasing temperature. This result is consistent with the work of Tani et al. [16] and Zhao et al. [2]. The carriers scattering by excess Si is sensitive at below 450 °C [17]. At high temperature, number of carriers increase so the influence of excess Si becomes insensitive. Peaks in the thermoelectric power generally appear near or above 330 °C in  $\text{FeSi}_{2.0}$  depending on

the processing method, such as in hot pressed [18], and in pressureless sintering [17]. In this work, the maximum thermoelectric power for  $\text{FeSi}_{2.0}$  is  $175 \mu\text{V/K}$  at  $500^\circ\text{C}$ . For  $\text{FeSi}_{2.3}$  and  $\text{FeSi}_{2.5}$ , the maximum thermoelectric power are  $240 \mu\text{V/K}$  and  $337 \mu\text{V/K}$  at  $400^\circ\text{C}$ , respectively

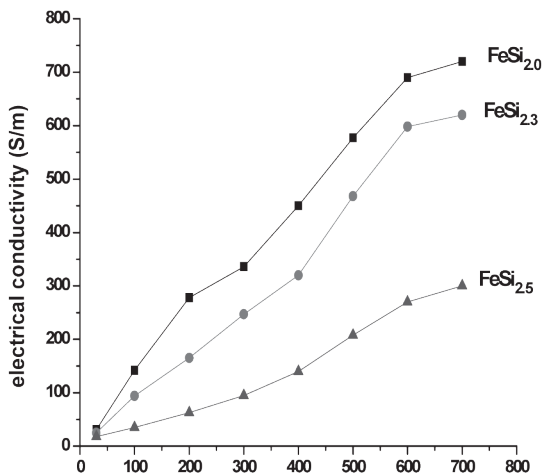


Figure 8: Temperature dependence of electrical conductivity of  $\text{FeSi}_{2.0}$ ,  $\text{FeSi}_{2.3}$  and  $\text{FeSi}_{2.5}$ .

Figure 8 shows the temperature dependence of electrical conductivity for annealed samples over the temperature range  $30\text{--}700^\circ\text{C}$ . The electrical conductivity of all samples increases rapidly with increasing temperature. The electrical conductivity of  $\text{FeSi}_{2.0}$  is higher than  $\text{FeSi}_{2.3}$  and the electrical conductivity of  $\text{FeSi}_{2.3}$  is higher than  $\text{FeSi}_{2.5}$ . These can be explained by the influence of metallic  $\epsilon$ -phase as present in the  $\text{FeSi}_{2.0}$  and  $\text{FeSi}_{2.3}$  samples. The calculated power factor from thermoelectric power and electrical conductivity are shown in Fig.9.

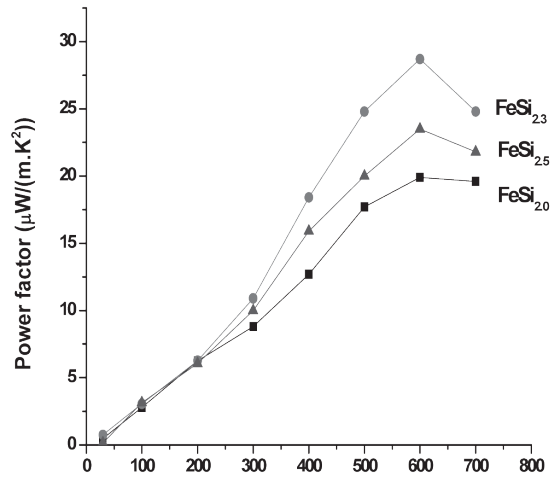


Figure 9. Temperature dependence of power factor of  $\text{FeSi}_{2.0}$ ,  $\text{FeSi}_{2.3}$  and  $\text{FeSi}_{2.5}$ .

The power factor of all samples increases with increasing the temperature and passes through the maximum point at the temperature of  $600^\circ\text{C}$ . The maximum power factor is  $2.86 \times 10^{-5} \text{ W}/(\text{m.K})$  obtained from  $\text{FeSi}_{2.3}$  sample. For  $\text{FeSi}_{2.0}$  and  $\text{FeSi}_{2.5}$  samples, the maximum power factor are  $1.99 \times 10^{-5} \text{ W}/(\text{m.K}^2)$  and  $2.34 \times 10^{-5} \text{ W}/(\text{m.K}^2)$ , respectively. In the case of  $\text{FeSi}_{2.5}$  sample, although it shows maximum thermoelectric power due to existence of excess Si. The  $\text{FeSi}_{2.5}$  sample shows very low electrical conductivity compared with  $\text{FeSi}_{2.0}$  and  $\text{FeSi}_{2.3}$  samples. In this work, the results indicate that the small metallic  $\epsilon$ -phase and excess Si in  $\text{FeSi}_{2.3}$  sample markedly increase the power factor.





#### 4. Conclusions

Fe–Si compounds were synthesized by thermal method and subsequent annealing. The microstructure and thermoelectric properties of FeSi<sub>2.0</sub>, FeSi<sub>2.3</sub> and FeSi<sub>2.5</sub> were investigated. Peritectoid and eutectoid reactions of Fe–Si compound were observed by DTA. The eutectoid reaction occurred in all samples. The peritectoid and its reverse reactions occurred in samples FeSi<sub>2.0</sub> and FeSi<sub>2.3</sub>. The  $\beta$ -phase formation was enhanced by annealing. The  $\beta$ -phase formation from peritectoid reaction gave the ring-like structure surrounding  $\epsilon$ -phase. This suggests that the peritectoid reaction rate increase with increasing the interface area between the  $\epsilon$  and  $\alpha$  phase. SEM image of sample FeSi<sub>2.5</sub> showed Si dispersed in the  $\beta$  matrix. The dispersion of excess Si markedly increased the thermoelectric power of both FeSi<sub>2.3</sub> and FeSi<sub>2.5</sub> samples especially at low temperature (less than 400 °C) while the present of metallic  $\epsilon$ -phase markedly increased the electrical conductivity of both FeSi<sub>2.0</sub> and FeSi<sub>2.3</sub> samples. The maximum power factor for FeSi<sub>2.0</sub>, FeSi<sub>2.3</sub> and FeSi<sub>2.5</sub> samples are  $1.99 \times 10^{-5} \text{ W}/(\text{m.K}^2)$ ,  $2.86 \times 10^{-5} \text{ W}/(\text{m.K}^2)$  and  $2.34 \times 10^{-5} \text{ W}/(\text{m.K}^2)$ , respectively.

#### 5. Acknowledgement

This research was supported by the Institute for the Promotion of Teaching Science and Technology (IPST). The author would like to thank Assoc. Prof. Aree Wichainchai for helpful.

#### 6. References

- [1] Birkholtz U. and Schelm J. (2006). Mechanism of electrical conduction in  $\beta$ -FeSi<sub>2</sub>, *Physica Status Solidi*, vol. 27(1), pp.413–425.
- [2] Zhao X.B., Zhu T.J., Hu S.H., Zhou B.C. and Wu Z.T. (2000). Transport properties of rapid solidified Fe–Si–Mn–Cu thermoelectric semiconductor alloy, *Journal of Alloys and Compounds*, vol. 306(1–2), pp. 303–306.
- [3] Sakata T., Sakai Y., Yoshino H., Fuji H. and Nishida I. (1978). Studies on the formation of FeSi<sub>2</sub> from the FeSi–Fe<sub>2</sub>Si<sub>5</sub> eutectic, *Journal of Less Common Metals*, vol. 61(2), pp. 301–308.
- [4] Yamauchi I., Ueyama S. and Ohnaka I. (1996).  $\beta$ -FeSi<sub>2</sub> phase formation from a unidirectionally solidified rod-type eutectic structure composed of both  $\alpha$  and  $\epsilon$  phases, *Materials Science and Engineering: A*, vol. 208, pp. 108–115.
- [5] Yamauchi I., Suganuma A., Okamoto T. and Ohnaga I. (1997). Effect of copper addition on the  $\beta$ -phase formation rate in FeSi<sub>2</sub> thermoelectric materials, *Journal of Materials Science*, vol. 32, pp. 4603–4611.
- [6] Umemoto M. (1995). Preparation of thermoelectric  $\beta$ -FeSi<sub>2</sub> doped with Al and Mn by mechanical alloying, *Material Transactions JIM*, vol. 36, pp. 373–383.
- [7] Ur S.C. and Kim I.H. (2002). Phase transformation and thermoelectric properties of n-type Fe<sub>0.98</sub>Co<sub>0.02</sub>Si<sub>2</sub> processed by mechanical alloying, *Material Letters*, vol. 57, pp. 543–551.

- [8] Nagai H. (1995). Effects of mechanical alloying and grinding on the preparation and thermoelectric properties of  $\beta$ -FeSi<sub>2</sub> (overview), *Material Transactions JIM*, vol. 36, pp. 363–372.
- [9] Ohta Y., Miura S. and Mishima Y. (1999). Thermoelectric semiconductor iron disilicides produced by sintering elemental powders, *Intermetallics*, vol. 7, pp.1203–1210.
- [10] Ito M., Nagai H., Tanaka T., Katsuyama S. and Majima K. (2001). Thermoelectric performance of n-type and p-type  $\beta$ -FeSi<sub>2</sub> prepared by pressureless sintering with Cu addition, *Journal of Alloys and Compounds*, vol. 319, pp. 303–311.
- [11] Nagai H., Katsuyama S., Ito M. and Majima K. (1998). Thermoelectric properties of  $\beta$ -FeSi<sub>2</sub> mechanically alloyed with Si and C, *Material Transactions JIM*, vol. 39, pp. 1140–1145.
- [12] Ito M., Tada T. and Katsuyama S. (2003). Thermoelectric properties of Fe<sub>0.98</sub>Co<sub>0.02</sub>Si<sub>2</sub> with ZrO<sub>2</sub> and rare-earth oxide dispersion by mechanical alloying, *Journal of Alloys and Compounds*, vol. 350, pp. 296–302.
- [13] Yamauchi I., Okamoto H., Sugauma A. and Ohnaga I. (1998). Effect of Cu addition on the  $\beta$ -phase formation rate in Fe<sub>2</sub>Si<sub>5</sub> thermoelectric materials, *Journal of Materials Science*, vol. 33, pp. 385–394.
- [14] Ur S.C. and Kim I.H. (2005). Thermoelectric properties of mechanically alloyed iron disilicides consolidated by various processes, *Metals Materials International*, vol.11, pp. 301–308.
- [15] Liu Z.X. (2005). Doping of  $\beta$ -FeSi<sub>2</sub> films with boron and arsenic by sputtering and its application for optoelectronic devices, *Optical Material*, vol. 27, pp. 942–947.
- [16] Tani J. and Kido H. (2000). Hall effect and thermoelectric properties of FeSi<sub>x</sub>, *Journal of Applied Physics*, vol. 39, pp. 1054–1057.
- [17] Yamauchi I., Ueyama S. and Ohnaka I. (1996).  $\beta$ -FeSi<sub>2</sub> phase formation from a unidirectionally solidified rod-type eutectic structure composed of both  $\alpha$ - and  $\epsilon$ - phases, *Materials Science and Engineering:A*, vol. 208, pp. 108–115.
- [18] Kobabayashi M., Hijikata K. and Ido S. (1990). The composition dependence of some electrical properties of FeSi<sub>x</sub> thin films, *Japanese Journal of Applied Physics*, vol. 29, pp. 1118–1121.